Generation and High-Resolution Photoelectron Spectroscopy of Small Organic Radicals in Cold Supersonic Expansions

by **Stefan Willitsch**[a]), **John M. Dyke**[b]), and **Frédéric Merkt**[a])*

[a]) Laboratorium für Physikalische Chemie, ETH Zürich, CH-8093 Zürich
[b]) Department of Chemistry, University of Southampton, Southampton SO9 5NH, UK

This article is dedicated to Professor *Jack D. Dunitz* on the occasion of his 80th birthday

A general method of generating radicals in cold supersonic expansions in the gas phase is presented. The method relies on excimer laser photolysis of suitable precursor molecules in a thin quartz capillary mounted at the orifice of a pulsed gas nozzle and can easily be combined with vacuum-UV photoionization mass spectrometry and high-resolution photoelectron spectroscopy to study the reactivity and the rovibronic energy level structure of neutral radicals and their ions, as well as to determine highly accurate adiabatic ionization energies. The characteristics of the radical source are described in detail, and its performance is illustrated by mass spectrometric and high-resolution photoelectron spectroscopic investigations of NH_2, CH_2, CH_3, C_2H, C_2H_3, and C_2H_5. The radical source is not only suitable to produce cold samples (rotational temperature of *ca.* 30 K) of radicals of moderate reactivity, such as NH_2, CH_3, or C_2H_5, but it is also useful to prepare highly reactive radicals (*e.g.*, C_2H) for spectroscopic investigations.

1. Introduction. – The high reactivity of radicals in the gas phase represents a driving force for chemical processes in the earth's and other planetary atmospheres [1][2], in the interstellar medium [3–6], and in combustion processes [7][8]. Their high reactivity poses problems for laboratory experiments aimed at studying their structural and dynamic properties because free radicals tend to be consumed by chemical reactions before they can be observed. Over the 100 years that have passed since the first report of a free radical [9], an astonishing amount of scientific ingenuity and creativity have made free radicals in the gas phase accessible to mass spectrometric (MS) investigations [10][11] and high-resolution spectroscopic investigations in the microwave, infrared (IR), visible (VIS), and ultraviolet (UV) regions of the electromagnetic spectrum [12], which represent, for gas phase species, what X-ray crystallography and NMR spectroscopy represent for the investigation of solids and liquids [13–15].

The main methods currently used to generate radicals in the gas phase are microwave or electric discharges [16–20], photolysis [21–24], H-atom abstraction by halogen atoms [25–27], and pyrolysis [28–31]. Each of these methods has undergone continual refinement and, when possible, has been rapidly adapted for use in combination with supersonic gas jets [28][32] and with new spectroscopic techniques, recent examples being cavity ring-down spectroscopy [19][33][34] and pulsed-field-ionisation zero-kinetic-energy (PFI-ZEKE) photoelectron spectroscopy [24][35–37].

We report here on a very simple and surprisingly general method of producing rotationally cold samples of free radicals by photolysis in supersonic gas jets for studies

by vacuum ultraviolet (VUV) photoionization mass spectrometry and photoelectron (PE) spectroscopy. Our original interest in developing such a radical source was not so much motivated by our desire to study small free radicals as it was to study the ionised radical species, *i.e.*, small molecular ions, by high-resolution photoelectron spectroscopy. Indeed, if radicals represent key chemical species in low density environments, the same is true for the ionic species. For example, ions produced in hydrocarbon flames play important roles in determining the chemical products [7][38]. When considering the spectroscopic data available on small molecular ions, such as XH_n^+ and $X_2H_m^+$ (X = C, N, O; $n = 1-5$, $m = 1-7$) that are believed to play an important role in the chemistry of the interstellar medium [4][39], it is surprising to see that several of these ions are spectroscopically not known at all and that others are only known from a very limited number of bands of the IR spectrum [40–44].

The advantages of PFI-ZEKE PE spectroscopy to study molecular radicals and ions reside in the high-resolution of the technique compared to conventional He(I) PE spectroscopy and in its very high sensitivity, which originates from the fact that PFI-ZEKE photoelectrons can be detected with an efficiency of more than 50%. PFI-ZEKE PE Spectroscopy has recently become an important method to study molecular cations, despite its lower resolution compared with direct microwave, IR, and VIS spectroscopy because the spectroscopic information on ions is obtained following photoabsorption from a *neutral* molecule and does not suffer from intrinsic limitations on the particle density encountered when studying the charged species directly. Recent examples of the application of PFI-ZEKE PE spectroscopy to the study of the energy level structure of radicals and their ions are those of the methyl radical [35][45], the ammonium radical [36], the benzyl radical [46], the allyl radical [37], the propargyl radical [47], and the methylene radical [24][48]. The diatomic radicals OH [49], NH [50], and SH [51] have also been studied by high-resolution PE spectroscopy. Two recent review articles summarise this progress [52][53].

If a correction is introduced for the field-induced shift of the ionisation thresholds, the adiabatic ionisation potentials of the radicals can be determined by PFI-ZEKE PE spectroscopy with an absolute accuracy of *ca.* 0.1 meV, provided the field ionisation dynamics of the *Rydberg* states during the electric-field pulse sequence is carefully taken into account [54]. This accuracy has led recently to a substantial improvement in the determination of key thermochemical quantities, such as heats of formation and bond dissociation energies of important intermediates in combustion processes [26][55–58].

Because of an insufficient knowledge of the electronically excited states of the radicals, or because possible intermediate states may be dissociative, direct single-photon VUV ionisation represents the most general and easily applicable method to study radicals by mass spectrometry and PE spectroscopy. Most of the successful investigations of radicals by photoionisation reported to date have, thus, relied either on VUV photoionisation mass spectrometry [11][26] or on VUV PE spectroscopy [27][59][60]. Nonresonant multiphoton ionisation does not require the existence of suitable intermediate electronic states either and has also been applied successfully to study radicals [47].

The following criteria can be formulated for a radical source designed for studies by high-resolution PE spectroscopy:

1) the source should be compatible with the high-vacuum environment required by VUV PE spectrometers
2) the source should produce cold radicals to avoid spectral congestion in the PE spectra and enhance the sensitivity (spectral congestion rapidly leads to a loss of the rotational fine structure and, hence, of precious structural information on the radical and its ion)
3) the source must be generally applicable and have the ability to generate highly reactive radicals
4) the source must be easy to maintain and operate stably.

Several of these requirements are met by existing radical sources, such as the flash pyrolysis source developed by *Chen* and co-workers [28][61] or the H-abstraction source used in photoionisation and PE-spectroscopic studies performed by *Ruscic* and co-workers [26], as well as by *Dyke* and co-workers [27][59].

This artice presents progress in the development of a source of cold radicals integrated in a high-resolution VUV PE spectrometer. This combination represents, in our opinion, a very general and attractive way of studying radicals and their ions.

2. Principle of Radical Generation and Apparatus. – The main features of the experimental procedure are *a*) the generation of cold radicals in a supersonic expansion by excimer-laser photolysis of suitable precursors in a quartz capillary, *b*) the photoionisation and the identification of the radicals by means of a VUV-laser radiation source and mass spectrometry, and *c*) the spectroscopic characterisation of the radicals by high-resolution single-photon PFI-ZEKE PE spectroscopy. In the following, these three parts of our procedure are described in detail. An overview of the apparatus is given in *Fig. 1.*

2.1. *Generation of Radicals.* Radicals are generated by excimer-laser photolysis of suitable precursor molecules R–X according to *Eqn. 1:*

$$R{-}X \rightarrow R^{\bullet} + N^{\bullet} \quad (1)$$

where $R^{\bullet}$ represents the radical to be studied and $X^{\bullet}$ the fragment radical produced in the homolytic bond breaking. In general, the excimer-laser photon energies lie significantly higher than the R–X bond dissociation energy, and the radicals are produced with a substantial degree of translational and internal energy.

To generate significant concentrations of cold radicals in a supersonic beam (the cooling necessitates collisions during the adiabatic expansion into the vacuum by which the radicals may be destroyed), a compromise has to be reached between optimum cooling, which requires many collisions in the high-pressure zone of the expansion, and maximum radical concentrations in the collision-free part of the expansion, which requires as few collisions as possible during the expansion. A satisfactory compromise can usually be found for radicals of low reactivity, but is very difficult to achieve for highly reactive radicals, such as C_2H or CH_2.

To be able to adapt the number of collisions in the expansion to the reactivity of the radicals, the photolysis is performed in a capillary (diameter 1 mm, length 25 mm) mounted at the orifice of a commercial, pulsed gas nozzle (*General Valve*, *Series 9*, 1-mm diameter orifice). The photolysis laser beam crosses the capillary at right angles,

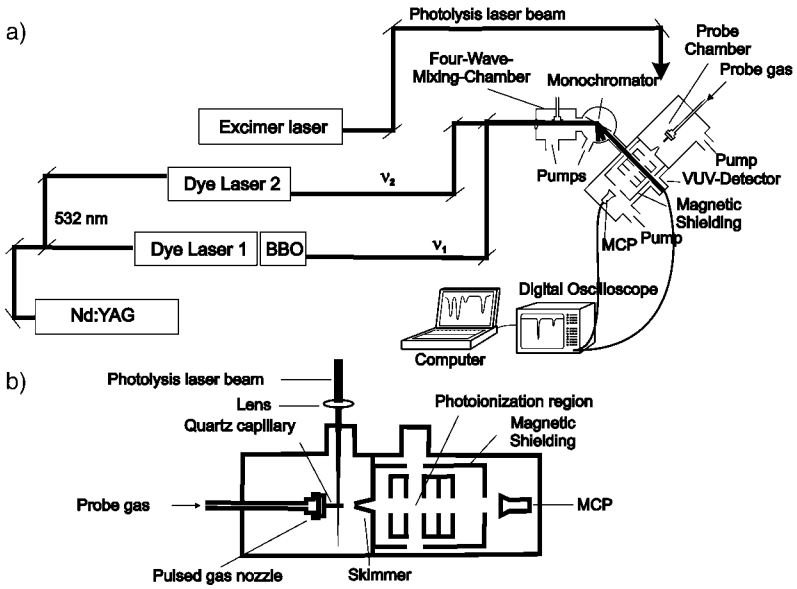

Fig. 1. a) *Schematic diagram of the experimental setup with the VUV laser system, the photodissociation and photoionisation regions, and the data-acquisition system*. b) *Enlarged view of the radical source and the photoionisation region.*

and the number of collisions the radicals undergo before they enter the collision-free part of the expansion at the end of the capillary can be adjusted freely by moving the position of the excimer beam along the capillary axis. For the capillary material, fused silica was chosen, because fused silica transmits UV radiation at most commonly used excimer-laser wavelengths, except 157 nm.

The pulsed excimer-laser source (*Lambda Physik*, *Compex 102*, 10-Hz repetition rate) can be operated at different wavelengths (351 nm, 308 nm, 248 nm, and 193 nm). Photolysis at 193 nm turned out to be particularly advantageous because *a*) most radical precursors R–X with X = Cl, Br, or I possess substantial absorption cross-sections at this wavelength and *b*) the photon energy is sufficient to break almost any chemical bond. Other photolysis wavelengths can be used whenever one desires to discriminate energetically against unwanted dissociation products or to achieve a good match with a strong absorption band of the precursor.

The photolysis laser beam is weakly focused into the capillary (laser spot size 2 mm × 4 mm, pulse energy 20 mJ) so that the capillary is not optically damaged, and the conditions are mild enough that the capillary remains transparent over extended experimental periods (several weeks). The selection of the cold part of the supersonic expansion is achieved by means of a skimmer (*Beam Dynamics*, *Model 2*, 0.5 mm diameter) placed 20 mm away from the capillary (see *Fig. 1*, *b*).

When the investigation of a 'warm' sample is desired, the photolysis can be performed in the collision-free region behind the skimmer, preferably in, or as close as possible to the photoionisation region.

The collisions taking place in the capillary and in the high-pressure zone of the expansion inevitably lead to the formation of some reaction products. Although these represent an unwanted complication in spectroscopic experiments, the mass-spectrometric analysis of the products provides useful information on the reactivity of the radicals and on the performance of the radical source. They can also facilitate the identification of the best position of the photolysis beam in the capillary.

2.2. *Identification of the Radicals by VUV Photoionisation Mass Spectrometry.* To identify the radicals produced by photolysis, photoionisation mass spectrometry is used. Single-photon photoexcitation with a VUV radiation source represents the most general way of ionising radicals. Our VUV laser source [62][63] is broadly tunable between 150 and 63 nm (8–19.5 eV), with a bandwidth of 0.1 cm^{-1}, and is based on resonance-enhanced four-wave mixing in atomic rare-gas beams. For the experiments described here, Xe was used as the nonlinear medium, and VUV radiation with wavenumber $\tilde{\nu}_{VUV} = 2\tilde{\nu}_1 + \tilde{\nu}_2$ was generated by sum-frequency mixing of the output of two pulsed dye lasers of wavenumber $\tilde{\nu}_1$ and $\tilde{\nu}_2$, respectively. The resonance enhancement of the sum-frequency mixing was achieved by fixing the wavenumber of the first dye laser to the position of the $(5p)^5\ (^2P_{3/2})6p[1/2](J=0) \leftarrow (5p)^6\ ^1S_0$ two-photon resonance of Xe at $2\tilde{\nu}_1 = 80119\ cm^{-1}$. Tunability in the VUV, when required, was achieved by scanning the wavenumber $\tilde{\nu}_2$ of the second dye laser.

A monochromator equipped with a Pt-coated toroidal grating is employed to separate the sum-frequency radiation from the fundamental beams ($\tilde{\nu}_1$ and $\tilde{\nu}_2$) and from the radiation produced by other nonlinear processes (*e.g.*, the third harmonic $3\tilde{\nu}_1$). The toroidal geometry of the grating also recollimates the diverging VUV radiation and redirects it towards the photoionisation region where it intersects the skimmed supersonic probe-gas expansion at right angles in the middle of a set of equidistant cylindrical electrodes. After the monochromator, the VUV pulse energy amounts to 10^{10} photons (*i.e.*, *ca.* 20 nJ) in the range 93000–105000 cm^{-1}, which, at the 10-Hz repetition rate of the experiment, corresponds to an average power of 0.2 μW.

Because of their short duration (*ca.* 5 ns), the VUV laser pulses are well-suited to define the time origin of the experimental cycles and of the time-of-flight (TOF) spectra. These are recorded after each laser shot by extracting all ions produced by the VUV radiation with a 350 V/cm electric field (dc) towards a microchannel plate detector placed at the end of a short flight tube. The mass resolution $m/\Delta m$ of our linear mass spectrometer lies above 200, which is sufficient to distinguish radicals from their precursors even when they differ by only one H-atom. In general, four types of ions are produced by VUV photoionisation that contribute to the TOF mass spectra: the precursor ions, the ions of the radicals generated by the photolysis, the ionised products of the radical reactions taking place in the gas expansion, and, finally, the fragment ions produced by dissociative ionisation of either the precursor or the photolysis or reaction products. The ions generated by either direct ionisation or dissociative ionisation of the precursor are produced independently of the photolysis laser.

To be able to detect both the radicals and their potential reaction products (some of which have ionisation energies substantially higher than the radicals) by photoionisation MS, it is advantageous to use short-wavelength VUV radiation when first characterising the operation of the radical source. To meet this requirement for the small radicals of interest, radiation of 100000 cm^{-1} (wavelength 100 nm) was found to

be particularly convenient. The drawback of using short-wavelength radiation lies in the fact that the first dissociative ionisation threshold of the precursor

$$R{-}X \rightarrow R^{+} + X^{\cdot} + e^{-} \qquad (2)$$

may lie below this photon energy, leading to a photolysis-independent ion signal at the mass of the radical.

For the success of the experiment, it is crucial to carefully optimise the time difference between the photolysis and VUV laser pulses to exactly match the time needed by the radicals to travel from the photolysis region to the photoionisation region. Gas samples in which the precursors are strongly diluted in the carrier gas (Ar was used in all our experiments) offer the advantage that the time difference becomes independent of the radical/precursor pair under study and needs to be determined only once.

TOF Mass spectrometry was also useful in identifying disturbances in the gas flow in the capillary induced by excimer-laser photolysis. Indeed, the observation was made that both the radical and precursor VUV ionisation signals were dependent on the time delay between the photolysis and the VUV laser pulses. As an illustration, *Fig. 2* shows TOF mass spectra near the position of the CH_3I^+ mass peak obtained in an expansion of a Ar/CH_3I 50 : 1 mixture exposed to photolysis at 193 nm in the capillary. Panels *a*–*e* display the CH_3I^+ signal at different delay times between the photolysis and VUV laser pulses, and panel *f* shows the same signal when the photolysis laser is turned off. The measurement points in panel *g* represent the integrated CH_3I^+-signal intensity as a

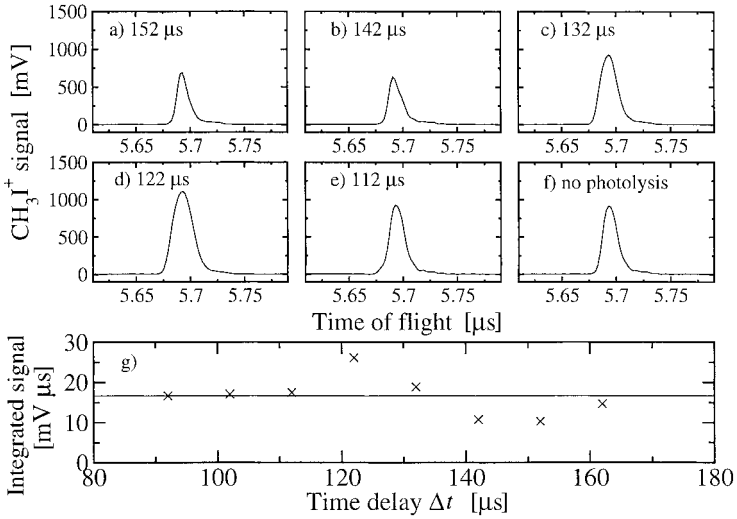

Fig. 2. *TOF Mass spectra in the region of the CH_3I^+ mass peak*. Photoionisation was carried out at a wavenumber of 101 000 cm^{-1}. Traces *a*–*e* were obtained at different delays Δt between the 193-nm photolysis and photoionisation laser pulses. a) $\Delta t = 152$ μs, b) $\Delta t = 142$ μs, c) $\Delta t = 132$ μs, d) $\Delta t = 122$ μs, and e) $\Delta t = 112$ μs. Trace *f* shows the CH_3I^+ signal recorded with the photolysis laser turned off. Panel *g* displays the integrated signal intensity as a function of Δt, the signal level without photolysis being indicated by the horizontal line.

function of the delay time, which, in selected ranges, can even become larger than when the photolysis is turned off (the horizontal line in *g* indicates the signal strength without photolysis). Similar behavior was also observed in experiments carried out on the other precursors: NH_3, C_2H_5I, HC_2I, and C_2H_3Br. The variation in the CH_3I^+ signal is attributed to particle density fluctuations in the capillary caused by local heating at the focus of the excimer-laser beam and by the local pressure increase resulting from the photodissociation. Particularly noteworthy is the observation that a maximum CH_3I^+ signal is observed at the time delay of 122 μs, despite the fact that, at this delay time, the amount of dissociation products is also close to its maximum.

2.3. *Characterization of the Radicals by High-Resolution PFI-ZEKE Photoelectron Spectroscopy.* The PFI-ZEKE PE spectra are obtained by monitoring the field ionisation of very high *Rydberg* states (principal quantum number $n \gg 200$) located just below each ionisation threshold by delayed pulsed-field ionisation as a function of the VUV wavenumber. Each ionisation threshold corresponds to an energy difference between a quantum state of the ion and one of the neutral species. A resolution better than 1 cm^{-1} (the best resolution achieved to date by PFI-ZEKE PE spectroscopy is 0.06 cm^{-1} [54]) is amply sufficient to resolve the rotational structure in the PE spectrum of small radicals, allowing one to derive information on the energy level structure of both the neutral radicals and their ions.

PFI-ZEKE PE Spectra of the radicals are recorded in the same apparatus as used for the MS experiments described above, the only modification being that the voltages applied on the cylindrical electrodes and the microchannel plates are changed. A double layer of μ-metal shielding surrounds the TOF tube and ensures an optimal detection efficiency of the PFI-ZEKE photoelectrons.

The pulsed electric-field sequence used to record PFI-ZEKE PE spectra of radicals consists of a double pulse with a first discrimination pulse of 170 mV/cm (used to eliminate background electrons and electrons produced by direct ionisation) and a second detection pulse of − 520 mV/cm. This pulse sequence enables a resolution of 1.0 cm^{-1} to be reached in the photoelectron spectra of radicals, and the adiabatic ionisation energies of the radicals to be measured with an absolute accuracy of $\pm$ 1 cm^{-1} (0.1 meV). Although a higher resolution can be obtained with other pulse sequences [54], this sequence offers the advantage of a particularly high sensitivity, which can be decisive in the study of radicals that are often present in only small partial pressures in the probe-gas sample.

3. Characterization of the Radical Source by Mass Spectrometry and High-Resolution Photoelectron Spectroscopy. – In this section, the operation characteristics of the radical source are illustrated by examples ranging from moderately reactive radicals, such as NH_2 to highly reactive radicals, such as C_2H. The emphasis is placed on the mass-spectrometric characterization of the radicals and the reaction products they form before they reach the collision-free region of the supersonic expansion. High-resolution PE-spectroscopic results are only shown here to demonstrate the low rotational temperature of these species reached in the supersonic expansion and the feasibility of combining the radical source with PFI-ZEKE photoelectron spectroscopy.

3.1. *The Amidogen Radical* (NH_2) *from the 193-nm Photolysis of Ammonia.* The photodissociation of NH_3 following excitation to the $\tilde{A}$ state, for instance by 193-nm

radiation, represents one of the most extensively studied photoinduced reactions [64–66]. This excitation wavelength corresponds to a strong absorption to the predissociative $\tilde{A}$ state of ammonia and can be used to produce the amidogen radical very efficiently [67]. The NH_2 fragments are produced with a considerable amount of internal excitation. The preferential population of the highest N and K_a asymmetric top rotational levels of the $\tilde{X}\ ^2B_1$ ground-state of NH_2 leads to a strongly nonequilibrium and unusually broad distribution of rotational-state populations. The broad distribution of the population over many quantum states results in a marked reduction in the sensitivity of high-resolution spectroscopic measurements. The 193-nm photolysis of NH_3, thus, provides a stringent test for the cooling efficiency of the supersonic expansion leaving our capillary radical source.

In *Fig. 3*, the TOF mass spectra obtained *with* (trace *b*) and *without* (trace *a*) photolysis are compared. Only NH_3^+ is observable in the latter spectrum, while the former reveals a photolysis-dependent decrease of the NH_3^+ signal and the associated appearance of the amidogen ion. The effect of the photolysis laser is illustrated more clearly by trace *c*, which represents the difference between traces *b* and *a*, a negative signal indicating a depletion of population (in the remainder of this article, such difference mass spectra will be used to discuss the effects of the photolysis). A striking aspect of *Fig. 3* is the selectivity of the radical-generation process, which only leads to minor contributions from reaction products to the TOF mass spectra (see magnified inset above trace *c*). An increase of the photolysis intensity did not enhance the NH_2^+ signal, primarily because of the (multiphoton) ionisation and dissociation of the radical by the 193-nm radiation.

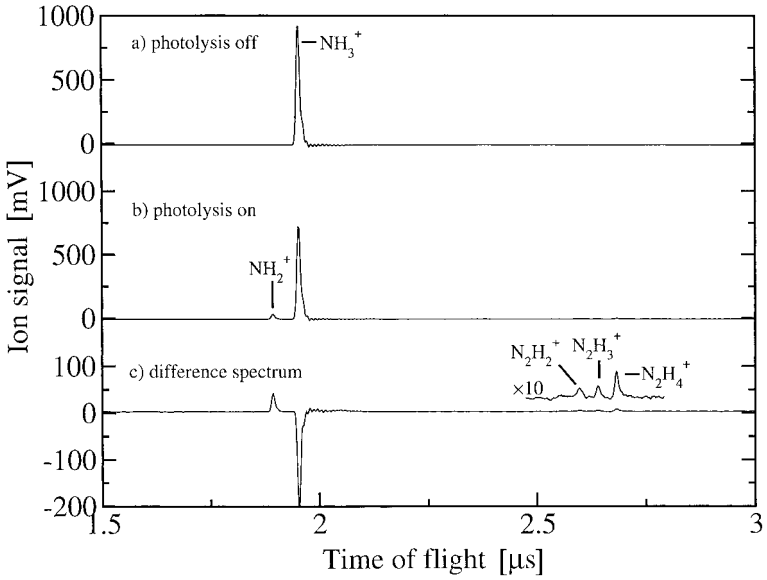

Fig. 3. *TOF Mass spectra illustrating NH_2-radical generation by 193-nm photolysis of NH_3. a*) Mass spectrum following photoionisation of NH_3 at 100500 cm^{-1}. *b*) As *a*, but with the 193-nm photolysis laser turned on. *c*) Difference mass spectrum obtained by subtracting trace *a* from trace *b*.

Although the yield of NH_2 is small, it is sufficient to record PFI-ZEKE photoelectron spectra with a satisfactory signal-to-noise ratio, as illustrated in *Fig. 4*, which shows a rotationally resolved PFI-ZEKE photoelectron spectrum of the origin band of the NH_2^+ $\tilde{a}\ ^1A_1 \leftarrow NH_2$ $\tilde{X}\ ^2B_1$ ionising transition. Analysis of the rotational structure of the spectrum reveals that only six rotational levels are significantly populated in the ground neutral state (the 0_{00}, 1_{01}, 1_{11}, 1_{10}, 2_{02}, and 2_{11} levels; the notation $N_{K_aK_c}$ indicates the asymmetric top rotational quantum numbers). The observed intensity distribution is consistent with a simulation of the spectrum assuming a *Boltzmann* distribution with a rotational temperature $T_{rot} = 30$ K (see bottom trace in *Fig. 4*). The weak transitions marked by asterisks at the right of the figure can be assigned to transitions to a highly excited vibrational level of the $\tilde{X}^3B_1$ electronic ground state of NH_2^+ and were not included in the simulation. The measurement displayed in *Fig. 4* represents the first determination of the rotational structure of singlet NH_2^+.

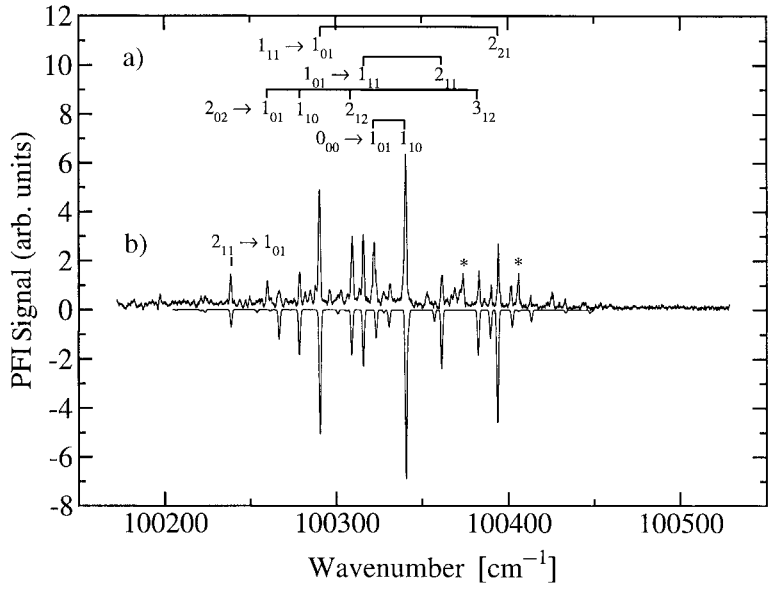

Fig. 4. *PFI-ZEKE Photoelectron spectrum of the origin of the* NH_2^+ $\tilde{a}\ ^1A_1 \leftarrow NH_2$ $\tilde{X}\ ^2B_1$ *transition. a*) Experimental spectrum. The assignment of the rotational structure is indicated along the assignment bars. The lines marked by asterisks correspond to transitions to a vibrationally excited level of the $\tilde{X}\ ^3B_1$ state of NH_2^+. *b*) Simulation of the spectrum assuming a *Boltzmann* distribution of rotational-state population with $T_{rot} = 30$ K.

The PFI-ZEKE photoelectron spectrum of NH_2 could not be detected when the photolysis was carried out in the photoionisation region (see *Fig. 1,b*), despite the fact that the NH_2^+ signal was almost five times larger than when the photolysis was carried out in the capillary. This observation nicely illustrates the advantage of an enhanced sensitivity resulting from the confinement of the population to a very limited number of quantum states by cooling the radicals in a supersonic jet.

3.2. *The Ethynyl Radical* (C_2H) *from the 193-nm Photolysis of Iodoacetylene*. The C_2H radical is highly reactive and was investigated here primarily to assess the suitability of our approach to generate cold reactive radicals. Photolysis of iodoacetylene at 193 nm was the production route selected. The absorption spectrum of iodoacetylene possesses a weak feature at 193 nm [68], but the dissociation dynamics of C_2HI at 193 nm are poorly characterised. The production of C_2H has been reported by *Blush et al.* [69] by pyrolysis of *tert*-butyl perpropriolate.

The difference TOF mass spectra (see *Sect. 3.1*) obtained by performing the photolysis at the tip of the capillary and in the middle of the capillary are displayed in *Figs. 5*,*a* and *b* respectively. Whereas the former spectrum reveals a clear C_2H^+ signal indicative of an efficient radical production, the latter does not show any such signal. Instead, a prominent series of peaks appear at the masses of recombination and other reaction products of C_2H (*e.g.*, C_4H_2, C_6H_2, C_8H_2), which indicates that the C_2H radicals produced by the 193-nm photolysis are destroyed by subsequent reactive collisions on their way to the exit of the capillary.

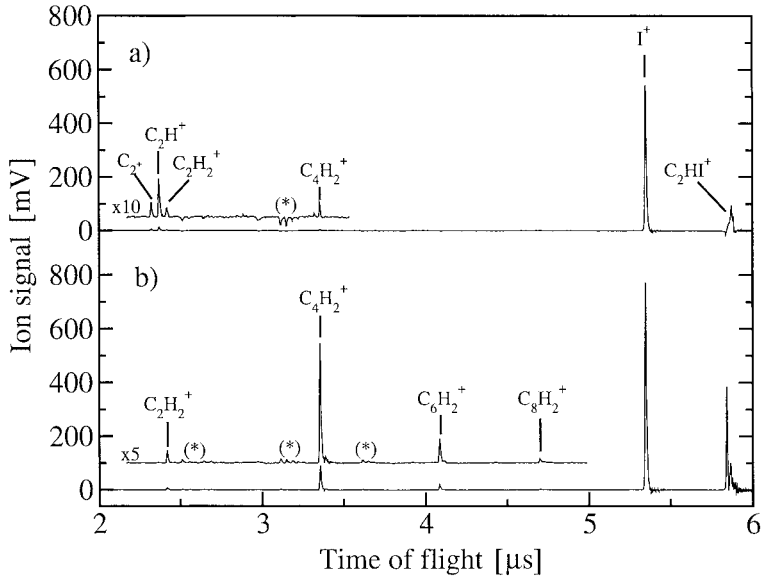

Fig. 5. *Difference mass spectra recorded following the 193-nm photolysis of iodoacetylene.* To record traces *a* and *b*, the photolysis laser crossed the capillary at its exit tip and in the middle position, respectively. The features designated by asterisks stem from impurities in the gas sample. The residual C_2HI^+ signal in the difference spectrum is an artifact caused by the saturation of the MCP detector. Photoionisation was carried out at a wavenumber of 101 000 cm^{-1}.

The reaction products are much less prominent in *Fig. 5*,*a*, and the comparison between *Figs. 5*,*a* and *b* clearly demonstrates our ability to control the number of collisions by displacing the photolysis beam along the capillary axis.

The efficiency of the photolysis is also documented by the dominant I^+ signal in the difference spectrum. No HI^+ stemming from the VUV photoionisation of HI is noticeable, which indicates that the H-abstraction reaction,

$$I + C_2HI \rightarrow HI + C_2I \quad (3)$$

is negligible. H-Abstraction by the halogen atom becomes important when the precursors are H-rich (see *Sect. 3.4*).

3.3. *The Methylene Radical* (CH_2) *from the 351-nm Photolysis of Ketene.* The photolysis of ketene at 351 nm exclusively leads to the formation of the $\tilde{X}\ ^3B_1$ ground-state of CH_2, dissociation to the first excited $\tilde{a}\ ^1A_1$ state being energetically inaccessible at this wavelength [70]. Moreover, the photolysis energy only slightly exceeds the dissociation energy, and only a few rotational levels of the ground vibronic state of CH_2 are populated [24][70]. In this case, no substantial advantage can be gained from freezing internal degrees of freedom in the supersonic expansion, and, in contrast to the situation encountered in the study of NH_2 (see *Sect. 3.1*), the PFI-ZEKE PE spectrum of CH_2 has been recorded by carrying out the photolysis in the photoexcitation region [24][48].

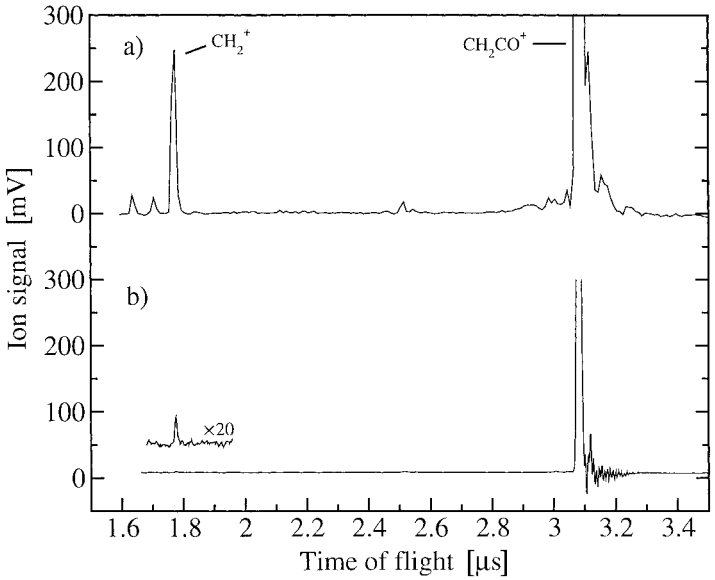

Fig. 6. *Comparison between TOF mass spectra obtained after the 351-nm photolysis of ketene.* To record traces *a* and *b*, the photolysis was performed in the photoexcitation region and the middle of the capillary, respectively. Photoionisation was carried out at a wavenumber of 101 000 cm^{-1}.

Carrying out the 351-nm photolysis in the capillary leads to a considerable loss of radical concentration, as demonstrated in *Fig. 6*, where the TOF mass spectra recorded after photolysis of CH_2CO in the photoionisation region (trace *a*) and in the capillary (trace *b*) are compared. In the latter case, the photolysis laser beam crossed the capillary 10 mm away from the exit. However, in contrast to the situation described above for the C_2H radical (see *Sect. 3.2*), no increase of the CH_2^+ signal could be achieved by displacing the photolysis laser towards the exit of the capillary, nor could significant amounts of recombination and polymerisation products be detected. Two conclusions can be reached from these observations: *1*) CH_2 in its $\tilde{X}\ ^3B_1$ ground state is

not destroyed by reactive collisions in the capillary and, thus, appears less reactive in the expansion than C_2H, and *2*) the radical yield is strongly reduced when the photolysis is carried out in the high-pressure zone. We interpret this second conclusion by collisional quenching of the 351-nm-excited ketene molecules before dissociation can take place. Dissociation is known to occur on a time scale of several tens of ns [71] because of the required intersystem crossing on the excited-state potential surfaces of ketene. Collisional quenching of all other precursor molecules investigated here could not compete with the photodissociation.

3.4. *The Methyl, Ethyl, and Vinyl Radicals from the 193-nm Photolysis of Monohalogenated Hydrocarbons.* Most monohalogenated hydrocarbons have significant absorption cross sections around 193 nm and readily dissociate into a halogen atom and the corresponding hydrocarbon radical [72][73].

Because an important aim of the present investigation was to identify the products of the radical reactions taking place in the capillary, MS experiments were carried out at a photon energy above the ionisation energy of the reaction products, but also above the first dissociative ionisation threshold of the precursor (see *Eqn. 2*). As a result, the ion signal at the mass of the radical could not be used as a diagnostic of radical production by photolysis. This problem is illustrated by *Fig. 7*, which presents the difference mass spectra obtained after the 193-nm photolysis of MeI (trace *a*), EtI (trace *b*), and vinyl bromide (trace *c*). In these spectra, the signal at the mass of the radical results from the difference of two very large signals because the VUV dissociative ionisation of the precursor is by far the dominant mechanism of production of the ionised radical. The signal-to-noise ratio of the difference mass spectra at the mass of the radical is insufficient to allow for even a qualitative analysis. However, the spectra supply sufficient indirect evidence that the radicals are produced (see below). Moreover, the greater stability of the radicals compared to C_2H also indirectly suggests that they survive until they reach the photoionisation region.

The observation of strong I^+ and HI^+ signals (or Br^+ and HBr^+ signals) in the difference spectra of *Fig. 7* represents the clearest evidence for efficient radical formation by 193-nm photolysis. The HI^+ and HBr^+ signals originate from H-abstraction from the precursor by the halogen (in analogy to *Eqn. 3*) followed by the VUV photoionisation of the HI or HBr products, and their magnitude appears to be proportional to the number of H-atoms in the precursor molecule.

The second evidence for radical production stems from the observation of radical reaction products in all three cases. The weakness of these signals compared to the strength of the I^+ or Br^+ and HI^+ or HBr^+ signals, however, clearly indicates that a large fraction of the radicals survive until reaching the photoionisation region. (In the case of C_2H, which is completely destroyed chemically under similar photolysis conditions (see *Fig. 5*,*b*), the recombination and other reaction products are much more prominent than in *Fig. 7*).

Also, the mere fact that a significant fraction of the halogen atoms, which are themselves reactive radicals, survive the supersonic expansion and live long enough to reach the photoexcitation region unscathed provides evidence for the versatility and the general applicability of our radical source.

4. Conclusions. – Excimer-laser photolysis in a quartz capillary mounted at the end of a pulsed gas nozzle represents a surprisingly simple and general method to generate

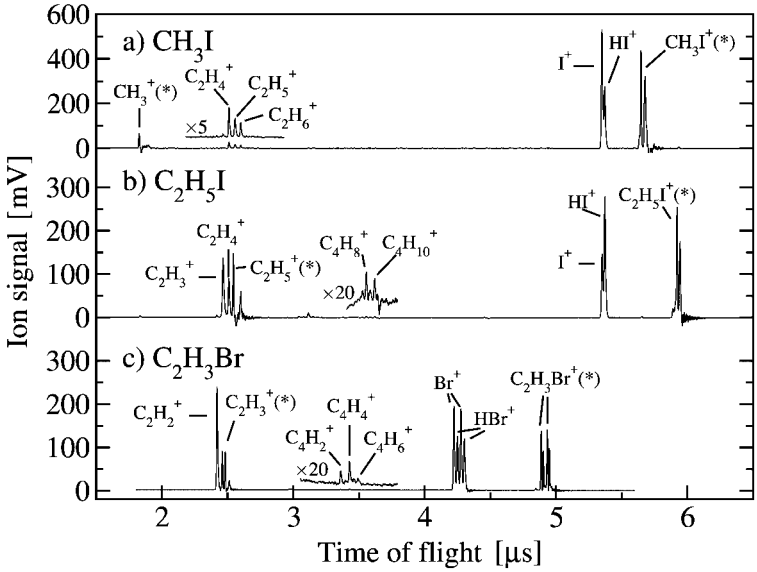

Fig. 7. *Difference mass spectra obtained following the 192-nm photolysis of CH_3I, C_2H_5I, and C_2H_3Br.* Photoionisation was carried out at a wavenumber of 101 000 cm^{-1}. The peaks marked by an asterisk originate from the subtraction of two very large signals and must be disregarded (see text for further details).

cold populations of radicals in supersonic gas jets. This method has been used to generate Br, I, NH_2, CH_2, CH_3, C_2H, C_2H_3, and C_2H_5 radicals. Moving the photolysis beam along the capillary axis enables one to adapt the expansion conditions to the reactivity of the radicals and offers a way to study even highly reactive species.

The pulsed, skimmed nature of the supersonic expansion makes the radical source easy to combine with a photoionisation mass spectrometer and/or a PE spectrometer. Moreover, the low rotational temperature of the radical population enables one to avoid spectral congestion and, thus, enhances the sensitivity of high-resolution spectroscopic measurements. The power of the combination of the radical source with high-resolution VUV PFI-ZEKE PE spectroscopy has been demonstrated by the recording of the first rotationally resolved spectrum of the singlet amidogen ion.

The new source of cold radicals described in this article adds to the diversity of methods of generating cold radicals and offers distinct advantages for the spectroscopic study of particularly reactive radicals.

We thank *Guido Grassi* (ETH Zürich) for help with the synthesis of ketene and iodoacetylene. *J. M. D.* thanks Prof. *Merkt* and his group for the hospitality during a short period of study leave at the ETH. This work was supported by the *Swiss National Science Foundation* and the ETH Zürich.

REFERENCES

[1] M. J. Prather, R. T. Watson, *Nature* **1990**, *344*, 729.
[2] R. P. Wayne, 'Chemistry of Atmospheres', 2nd edn., Oxford Science Publications, Oxford, 1991.
[3] I. W. M. Smith, *Chem. Soc. Rev.* **2002**, *31*, 137.

[4] E. Herbst, *Annu. Rev. Phys. Chem*. **1995**, *46*, 27.
[5] G. H. Herbig, *Annu. Rev. Astrophys.* **1995**, *33*, 19.
[6] A. Omont, *J. Chem. Soc., Faraday Trans.* **1993**, *89*, 2137.
[7] T. A. Cool, in 'Lasers and Mass Spectrometry', Ed. D. M. Lubman, Oxford University Press, Oxford, 1990, Vol. 1, p. 446–467.
[8] P. A. Berg, D. A. Hill, A. R. Noble, G. P. Smith, J. B. Jeffries, D. R. Crosley, *Combust. Flame* **2000**, *121*, 223.
[9] M. Gomberg, *J. Am. Chem. Soc.* **1900**, *22*, 757.
[10] C. A. Shalley, G. Hornung, D. Schröder, H. Schwarz, *Chem. Soc. Rev*. **1998**, *27*, 91.
[11] J. Berkowitz, *Acc. Chem. Res.* **1989**, *22*, 413.
[12] G. Herzberg, 'Molecular Spectra and Molecular Structure', Krieger, Malabar, 1991, Vols. I–III.
[13] J. D. Dunitz, 'X-Ray Analysis and the Structure of Organic Molecules', Verlag Helvetica Chimica Acta, Basel, 1995.
[14] R. R. Ernst, G. Bodenhausen, A. Wokaun, 'Principles of Nuclear Magnetic Resonance in One and Two Dimensions', Clarendon Press, Oxford, 1987.
[15] K. Wüthrich, 'NMR of Proteins and Nucleic Acids', Wiley Interscience, New York, 1986.
[16] P. C. Engelking, *Rev. Sci. Instrum.* **1986**, *57*, 2274.
[17] R. Schlachta, G. Lask, S. H. Tsay, V. E. Bondybey, *Chem. Phys.* **1991**, *155*, 267.
[18] D. T. Anderson, S. Davis, T. S. Zwier, D. J. Nesbitt, *Chem. Phys. Lett*. **1996**, *258*, 207.
[19] T. Motylewski, H. Linnartz, *Rev. Sci. Instrum*. **1999**, *70*, 1305.
[20] J. M. Dyke, N. Jonathan, A. Morris in 'Electron Spectroscopy', Eds. C. R. Brundle, A. D. Baker, Academic Press, London, 1979, Vol. 3, p. 189–229.
[21] G. Herzberg, J. W. C. Johns, *Proc. R. Soc. London, Ser. A* **1966**, *295*, 107.
[22] H. Petek, D. J. Nesbitt, D. C. Darwin, C. B. Moore, *J. Chem. Phys.* **1987**, *86*, 1172.
[23] J. Schleipen, J. J. ter Meulen, L. Nemes, M. Vervloet, *Chem. Phys. Lett*. **1992**, *197*, 165.
[24] S. Willitsch, F. Merkt, *J. Chem. Phys.* **2003**, *118*, 2235.
[25] S. T. Gibson, J. P. Greene, J. Berkowitz, *J. Chem. Phys.* **1985**, *83*, 4319.
[26] B. Ruscic, *Res. Adv. Phys. Chem*. **2000**, *1*, 39.
[27] M. C. R. Cockett, J. M. Dyke, H. Zamanpour, in 'Vacuum Ultraviolet Photoionization and Photodissociation of Molecules and Clusters', Ed. C. Y. Ng, World Scientific, Singapore, 1991, p. 43–99.
[28] P. Chen, S. D. Colson, W. A. Chupka, J. A. Berson, *J. Phys. Chem*. **1986**, *90*, 2319.
[29] J. R. Dunlop, J. Karolczak, D. J. Clouthier, *Chem. Phys. Lett*. **1988**, *151*, 362.
[30] J. M. Dyke, E. P. F. Lee, A. Morris, N. Jonathan, *J. Chem. Soc., Faraday Trans. 2* **1976**, *72*, 814.
[31] D. K. Bulgin, J. M. Dyke, N. Jonathan, E. Lee, A. Morris, *J. Electron Spectrosc. Relat. Phenom.* **1977**, *12*, 67.
[32] P. C. Engelking, *Chem. Rev.* **1991**, *91*, 399.
[33] C. D. Ball, M. C. McCarthy, P. Thaddeus, *J. Chem. Phys.* **2000**, *112*, 10149.
[34] M. D. Wheeler, S. M. Newmann, T. Ishiwata, M. Kawasaki, A. Orr-Ewing, *Chem. Phys. Lett*. **1998**, *285*, 346.
[35] J. A. Blush, P. Chen, R. T. Wiedmann, M. G. White, *J. Chem. Phys.* **1993**, *98*, 3557.
[36] R. Signorell, H. Palm, F. Merkt, *J. Chem. Phys.* **1997**, *106*, 6523.
[37] T. Gilbert, I. Fischer, P. Chen, *J. Chem. Phys.* **2000**, *113*, 561.
[38] T. G. Wright, A. M. Shaw, J. M. Dyke, *J. Phys. Chem*. **1995**, *99*, 14207.
[39] S. Viti, D. A. Williams, P. T. O'Neill, *Astron. Astrophys.* **2000**, *354*, 1062.
[40] M. Rösslein, C. M. Gabrys, M.-F. Jagod, T. Oka, *J. Mol. Spectrosc.* **1992**, *153*, 738.
[41] Y. Kabbadj, T. R. Huet, D. Uy, T. Oka, *J. Mol. Spectrosc.* **1996**, *175*, 277.
[42] C. M. Gabrys, D. Uy, M.-F. Jagod, T. Oka, *J. Phys. Chem*. **1995**, *99*, 15611.
[43] M.-F. Jagod, M. Rösslein, C. M. Gabrys, B. D. Rehfuss, F. Scappini, M. W. Crofton, T. Oka, *J. Chem. Phys.* **1992**, *97*, 7111.
[44] E. White, J. Tang, T. Oka, *Science* **1999**, *284*, 135.
[45] H. Dickinson, T. Chelmick, T. P. Softley, *Chem. Phys. Lett*. **2001**, *338*, 37.
[46] G. C. Eiden, F. Weinhold, J. C. Weisshaar, *J. Chem. Phys.* **1991**, *95*, 8665.
[47] T. Gilbert, R. Pfab, I. Fischer, P. Chen, *J. Chem. Phys.* **2000**, *112*, 2575.
[48] S. Willitsch, A. Haldi, F. Merkt, *Chem. Phys. Lett*. **2002**, *353*, 167.
[49] R. T. Wiedmann, R. G. Tonkyn, M. G. White, K. Wang, V. McKoy, *J. Chem. Phys.* **1992**, *97*, 768.
[50] E. de Beer, M. Born, C. A. de Lange, N. P. C. Westwood, *Chem. Phys. Lett*. **1991**, *186*, 40.
[51] C.-W. Hsu, D. P. Baldwin, C.-L. Liao, C. Y. Ng, *J. Chem. Phys.* **1994**, *100*, 8047.
[52] R. C. Shiell, T. G. Wright, *Annu. Rep. Prog. Chem., Sect. C* **2002**, *98*, 375.
[53] I. Fischer, *Int. J. Mass. Spectrom*. **2002**, *216*, 131.

[54] U. Hollenstein, R. Seiler, H. Schmutz, M. Andrist, F. Merkt, *J. Chem. Phys.* **2001**, *115*, 5461.
[55] J. A. Blush, H. Clauberg, D. W. Kohn, D. W. Minsek, X. Zhang, P. Chen, *Acc. Chem. Res.* **1992**, *25*, 385.
[56] B. Ruscic, M. Litorja, R. L. Asher, *J. Phys. Chem. A* **1999**, *103*, 8625.
[57] R. Signorell, F. Merkt, *J. Chem. Phys.* **1999**, *110*, 2309.
[58] S. Willitsch, L. Imbach, F. Merkt, *J. Chem. Phys.* **2002**, *117*, 1939.
[59] J. M. Dyke, N. Jonathan, A. Morris, *Int. Rev. Phys. Chem*. **1982**, *2*, 3.
[60] P. Chen, in 'Unimolecular and Bimolecular Reaction Dynamics', Eds. C. Y. Ng, T. Baer, I. Powis, John Wiley & Sons, Chichester, 1994, p. 371 – 425.
[61] D. W. Kohn, H. Clauberg, P. Chen, *Rev. Sci. Instrum.* **1992**, *63*, 4003.
[62] F. Merkt, A. Osterwalder, R. Seiler, R. Signorell, H. Palm, H. Schmutz, R. Gunzinger, *J. Phys. B: At. Mol. Opt. Phys.* **1998**, *31*, 1705.
[63] H. Palm, F. Merkt, *Appl. Phys. Lett*. **1998**, *73*, 157.
[64] J. Biesner, L. Schnieder, J. Schmeer, G. Ahlers, X. Xie, K. H. Welge, M. N. R. Ashfold, R. N. Dixon, *J. Chem. Phys.* **1988**, *88*, 3607.
[65] J. Biesner, L. Schnieder, G. Ahlers, X. Xie, K. H. Welge, M. N. R. Ashfold, R. N. Dixon, *J. Chem. Phys.* **1989**, *91*, 2901.
[66] M. N. R. Ashfold, R. N. Dixon, M. Kono, D. H. Mordaunt, C. L. Reed, *Phil. Trans. R. Soc. Lond.*, *Ser. A* **1997**, *355*, 1659.
[67] E. L. Woodbridge, M. N. R. Ashfold, S. R. Leone, *J. Chem. Phys.* **1991**, *94*, 4195.
[68] D. R. Salahub, R. A. Boschi, *Chem. Phys. Lett*. **1972**, *16*, 320.
[69] J. A. Blush, J. Park, P. Chen, *J. Phys. Chem*. **1989**, *111*, 8951.
[70] C. G. Morgan, M. Drabbels, A. M. Wodtke, *J. Chem. Phys.* **1996**, *105*, 4550.
[71] I.-C. Chen, C. B. Moore, *J. Phys. Chem.* **1990**, *94*, 263.
[72] R. A. Boschi, D. R. Salahub, *Mol. Phys.* **1972**, *24*, 289.
[73] W. H. Pence, S. L. Baughcum, S. R. Leone, *J. Phys. Chem.* **1981**, *85*, 3844.

Received February 8, 2003